

Induction Coupler Motion Primatives

Benjamin Reinhardt[†] and Mason Peck

Abstract—Can you move along a surface in space without propellant or physical contact? On-orbit servicing requires a robot to operate in close proximity to the surface of a target spacecraft in order to inspect, refuel, or repair it. Robotic operation in close proximity is difficult in space because spacecraft are fragile and often have poorly known, undamped dynamics. Current actuators for locomotion and grasping during on-orbit servicing require physical contact with the target (dangerous), propellant (expensive), or cooperation from the target (often infeasible.) This paper presents a new actuator - the induction coupler - that generates eddy-current forces between a robotic orbital inspector and the conductive exterior of its target. These forces allow the inspector to crawl along the surface of a target *without physical contact*. Sets of induction couplers composed of spinning arrays of permanent magnets can exert control forces and torques in all six rigid-body degrees of freedom by strategically repelling and shearing across the surface of the target. This paper uses an analytical model of eddy-current forces to simulate the set of manoeuvres necessary to generate the control forces and torques that can move and orient a robotic orbital inspector. Experiments on a low-friction test bed demonstrate a successful implementation of the actuator and verify the manoeuvres.

I. INTRODUCTION

On-orbit servicing (OOS) is a valuable but difficult robotic task[3][4][5]. Just as on earth, large assets like the International Space Station (ISS) or geostationary satellites experience wear and unexpected problems that require inspection, repair, or refuelling[7][13]. These tasks are well suited for robots because it is less dangerous and expensive to send an inspection vehicle to geostationary orbit or outside the ISS than a human spacewalker[1].

Manoeuvring close to a target is essential to OOS and is a particularly risky proposition on orbit. There are presently three methods for an inspector to manoeuvre close to the surface of its target: it can physically grapple the surface to pull itself along; it can use propellant and thrusters; or it can use cooperative, non-contacting electromagnetic systems installed both on the inspector and the target. Grappling has many potential risks in an uncertain, low-friction environment[8]. Propellant is expensive and can damage sensitive targets[6]. Cooperation is infeasible in many situations because most spacecraft launch without the necessary subsystems: spacecraft are *not* designed to be inspected or repaired by robots.

Fortunately, the ISS and most spacecraft are composed of aluminium plates, curves, and beams. By introducing a changing magnetic field, a robotic inspector can induce eddy

currents in these non-magnetic but conductive components and use the reaction force between the field and the currents for actuation[14]. These eddy-current forces have several terrestrial applications from trash separation [12] to maglev propulsion,[11][9] but have never been used in robotics or orbital contexts. Induction couplers are actuators that utilize these eddy-currents. Their ability to actuate near a target without propellant or mechanical contact can provide a completely new way to perform robotic locomotion and manipulation in space.

The first step towards an induction coupler locomotion system is to show how to produce actuation in each degree of freedom (DoF). What is it capable of given different states? Eddy-current forces depend both on the robot's pose and the geometry of the environment. Simulating general eddy-current forces is normally done with finite element analyses (FEA) [2]. FEA are unsuitable for dynamically modelling induction couplers for two reasons: they are both too slow to run at each time step and their mesh of nodes needs change with the geometry of the system. Paudel and Bird derived an extensible analytical solution for eddy-current forces near a flat plate that enables fast simulations of induction couplers[10].

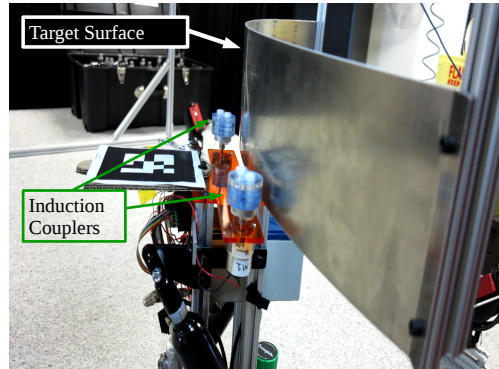


Fig. 1. An experimental inspector on a low-friction testbed uses induction couplers to actuate off of an aluminum plate simulating the ISS exterior.

This paper first extends the force model to find actuation forces for arbitrary configurations of multiple induction couplers. The model leads to four basic control inputs and their associated motion primitives that combined create 6-DoF actuation: planar forces (forces in the plane of the target), planar torques (torques about an axis out of the plane), out-of-plane forces, and out-of-plane torques. Each of these motions requires a different configuration of couplers and control input from those couplers. The intention of this paper is to demonstrate the raw capabilities of induction

[†] B. Reinhardt and M. Peck are with the Department of Mechanical Engineering at Cornell University, 127 Upson Hall, Ithaca, NY 14850
bzx3@cornell.edu

couplers and provide the motion primitives that will serve as the foundation of position controllers for robotic orbital inspectors.

Section II presents an analytical model to solve for induction coupler forces. Section III describes and simulates the necessary open-loop manoeuvres to move in each DoF. Finally, Section V presents experimental verification of each manoeuvre with a prototype induction coupler system on a low-friction testbed, shown in figure 1.

II. ACTUATOR MODEL

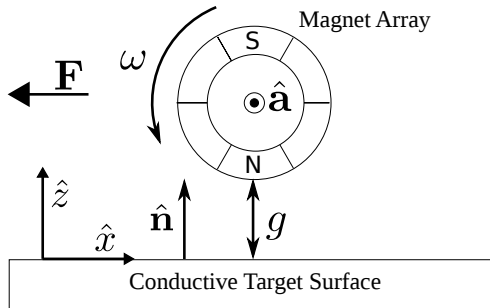


Fig. 2. Diagram of a single induction coupler array

Maxwell showed that time-varying magnetic field will induce an electric current in nearby conductors. Magnetic fields generate forces on moving currents, so these two effects combine to create eddy-current forces between a source of a changing magnetic field and a conductive surface. Induction couplers can use mechanically moving permanent magnets or time-varying electromagnets to generate a time-varying magnetic field. This paper focuses on the easiest and least power-intensive implementation of the mechanically-moving-magnet variety of induction coupler: a motorized, circular array of magnets.

Paudel and Bird derived an analytical solution for the force from a single rotating array of permanent magnets near a flat conductor. [10] In a reference frame attached to the conductive surface shown in figure 2, the force on the magnet array is

$$^s\mathbf{F} = \frac{w}{8\pi\mu_0} \int_{-\infty}^{\infty} \Gamma(\xi, g) |B^s(\xi, g)|^2 d\xi \quad (1)$$

where Γ is a transmission function associated with the conductive surface and B is the spatial Fourier transform of the time-invariant part of the array's magnetic field. Γ and B are nonlinear functions of the system state. Γ depends on the array's rotation frequency ω , velocity v and distance from the surface g . B is a nonlinear function of g as well. Near a curved surface, the assumption of an infinite flat surface is *locally* valid for induction couplers because the operating gap is on the order of centimeters: very small compared to the curvatures of most target surfaces.

Eddy-current properties and geometry can generalize this force for dynamic models of a 6-DoF orbital inspector. This

extension is important because the coupler's axis will rarely be perpendicular to the surface normal and it is much more convenient to calculate the forces in the inertial frame instead of a frame attached to the target surface. Eddy-current forces act only in opposition to change in magnetic field, so the net force will always act perpendicular to the array's spin axis. Thus, a 3D formulation of the force in any reference frame can be found by tilting the force plane (shown in figure 2 along with \hat{a} .)

$$\begin{aligned} \mathbf{F} = & F_z(g, \omega, \mathbf{v}) (\hat{a} \times \hat{n}) \\ & + F_y(g, \omega, \mathbf{v}) (\hat{a} \times \hat{n}) \times \hat{a} \end{aligned} \quad (2)$$

F_z and F_y are the components of the planar force calculated in equation 1.

This statement of eddy-current forces is powerful because it is both analytical and general. The generality enables fast simulations of a 6-DoF inspection vehicle while the analytical nature will enable provable statements about the system's stability. A full system consists of several couplers to control all six degrees of freedom. The net force and torque on the body then depends on the location and orientation of n arrays in the inspector's frame. Each coupler rotates around an axis, \hat{a}_n , located at \mathbf{d}_n , shown in figure 3. The net control force is

$$\mathbf{F}_{net} = \sum_i F_z(\hat{a}_i \times \hat{n}_i) + F_y(\hat{a}_i \times \hat{n}_i) \times \hat{a}_i \quad (3)$$

and the net control torque is

$$\tau_{net} = \sum_i \mathbf{d}_i \times [F_z(\hat{a}_i \times \hat{n}_i) + F_y(\hat{a}_i \times \hat{n}_i) \times \hat{a}_i] \quad (4)$$

\mathbf{n}_i is the vector to the surface segment closest to array i .

The following sections use this model to demonstrate how a robotic inspector can use induction couplers to generate forces and torques in all six rigid body degrees of freedom.

III. MOVEMENT PRIMITIVES

A. Planar Movement

While moving in the plane parallel to the target surface, induction couplers act similar to contactless wheels - they generate forces parallel to the surface that increase with their speed. Thus, a fixed arrangement needs at least two couplers to move in all three planar degrees of freedom and three couplers to control each degree of freedom independently. Unlike wheels, induction couplers do not provide constraint forces perpendicular to their rotation. They also cannot slip on the surface. So unlike wheels that skid if they accelerate too quickly, induction coupler forces are limited by the capabilities of their motors.

An inspector can translate in the plane by using a pair of induction couplers like differential drive wheels. Figure 3 shows this mode. Ideally, pure translational motion will involve no net torque. No net torque is difficult in practice because no kinematic constraints on the couplers make the system extremely sensitive to the relative location between the couplers and the system's center of mass (CoM). This sensitivity means that in open loop operation any unaccounted asymmetry between the two induction couplers will

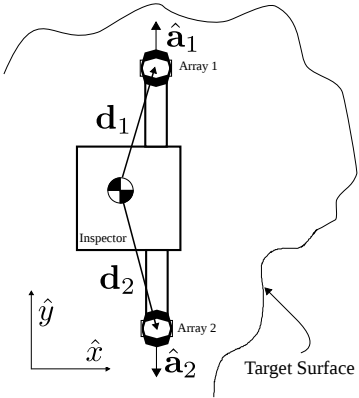


Fig. 3. Configuration for planar control: An inspector with two arrays spinning about \hat{y} can translate and rotate above a flat target surface

lead to unwanted torque. Thus, any induction coupler system will need closed-loop control.

An inspector also needs to rotate in the plane parallel to the surface. The simplest way for induction couplers to produce pure rotation is to act similarly to differential drive wheels with two couplers spinning in opposite directions on axes parallel to the surface. Like pure translation, pure rotation in a real system is sensitive to the relative geometry of the coupler, the surface, and the CoM location, again calling for wrapping a controller around these open loop manoeuvres.

B. Out-of-Plane Movement

It is more complicated for induction couplers to produce forces and torques that control movement out of the plane parallel to the target surface because the forces from a single induction coupler are limited in their direction.

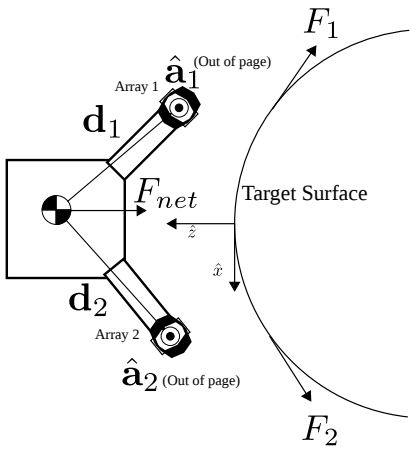


Fig. 4. Configuration for out-of-plane control

The forces generated by spinning magnets are almost completely tangential to the surface. For large ω , the ratio of the normal to tangential components of the force increases slightly and can be used to repel away from the surface. However, these forces are small and only act in the $+\hat{z}$ direction, giving no control in $-\hat{z}$. By strategically summing forces across several couplers near different locations on a

non-flat surface, the inspector can generate larger net forces in both $+\hat{z}$ and $-\hat{z}$.

Rotating two couplers oriented along the \hat{y} with opposing ω will create local forces whose \hat{x} components will cancel and whose \hat{z} components will sum, pulling the inspector towards the surface or pushing it away. This strategy is illustrated in figure 4.

Using locally tangential forces, the inspector can control rotation about the \hat{y} axis by giving each coupler the same input speed ω . With only two couplers, the torque will always come with a force - a third coupler would make the force and torque independent.

IV. SIMULATED DEMONSTRATION

In this section, simulations demonstrate each motion primitive - planar translation, planar rotation, out-of-plane translation, and out-of-plane rotation. In each case, the simulation constrains the inspector to the plane of interest to demonstrate open-loop motion primitives - in practice, a closed loop controller and more than two couplers are essential to account for motion out of the plane. The model inspector is the size of a small satellite using two motors each with two magnets as induction couplers. The parameters shown in table I match those used in the experimental demonstrations in section V.

TABLE I
SIMULATION PARAMETERS

Description	value	units
Max Coupler Speed, ω	32.7	rad s^{-1}
Max Coupler Power, P_{max}	2	W
Mass m	10.2	kg
Inertia J	1.02	kg m^2
Gap in Planar Movement g	1	cm
Conductivity, σ	2.5×10^7	Sm^{-1}
Curvature of non-flat target, κ	0.14	m^{-1}

A. Planar Movement

To demonstrate planar movement, the target is a flat plate in the x - y plane shown in figure 3. In a simulation of planar translation the inspector first drives itself forward by commanding opposite speeds in each coupler. Because $\hat{a}_1 = -\hat{a}_2$, opposite speeds in the couplers result in them both spinning in the same direction. The speeds of both couplers then reverse direction, creating a negative force and moving the inspector backwards. Figure 5 shows the coupler speeds, force, and displacement. In a simulation of planar rotation the inspector rotates commands the same speed to each coupler, rotating itself about the positive z axis. The speeds of both couplers then reverse direction, generating a torque about the negative z axis. Figure 6 shows the coupler speeds, torque, and heading.

B. Out-of-Plane Movement

To demonstrate out-of-plane movement, the target is a curved surface in the x - z plane, shown in figure 4. The

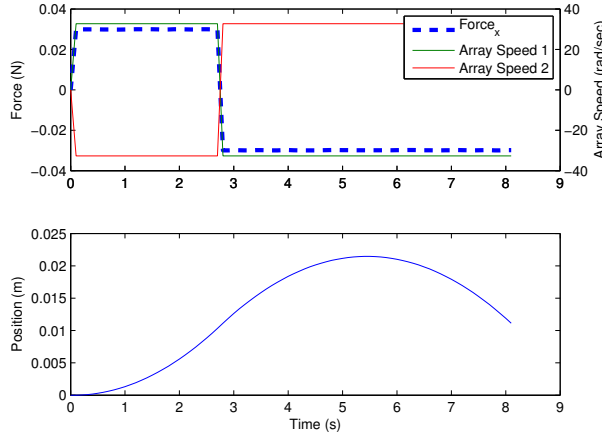


Fig. 5. Simulation of planar translation. The top plot shows the speed inputs to the couplers and resulting control force. The bottom plot shows the inspector's position

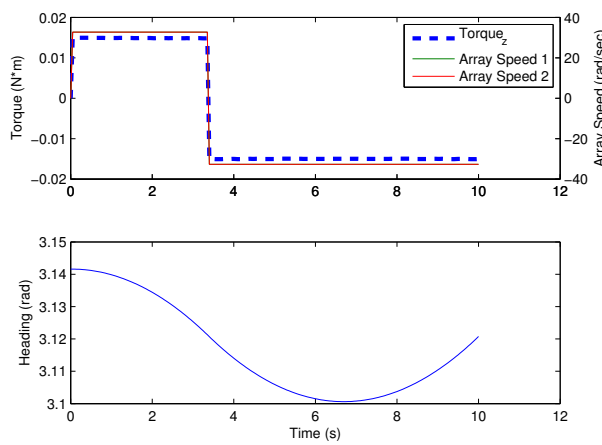


Fig. 6. Simulation of planar rotation. The top plot shows the speed inputs to the couplers and resulting control torque. The bottom plot shows the inspector's heading. Note: the control speed is the same for both arrays

surface curvature matches an ISS module both in simulation and experiment to approximate real capabilities as much as possible. The induction couplers both spin about the y axis in the body frame so that they can produce motion in the x-z plane by generating forces tangential to the surface.

In figure 7 the inspector pulls itself towards the surface by spinning with opposing speeds so that the z component of each tangential force is negative. When the forces from each coupler sum, the resultant force is entirely in the -z direction, pulling the inspector towards the surface. The inspector then reverses the coupler speeds, pushing itself away from the surface and preventing a collision. Finally, it stops itself at its original position.

In figure 8 the inspector rotates about the y axis by spinning each coupler in the same direction.

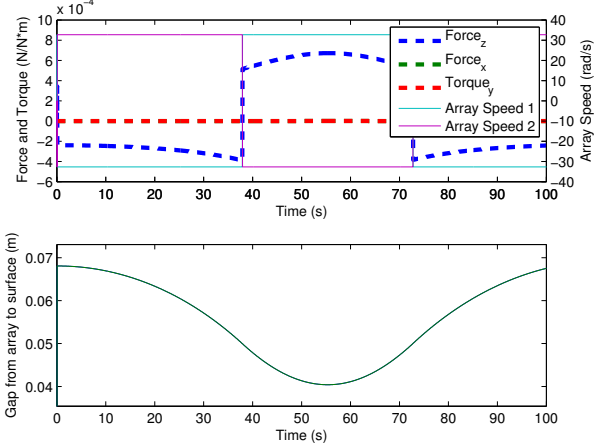


Fig. 7. Simulation of out-of-plane translation. The top figure shows the input speeds for each coupler and the resultant force on the inspector. The bottom figure shows how the gap between each coupler and the surface change in response to the control forces

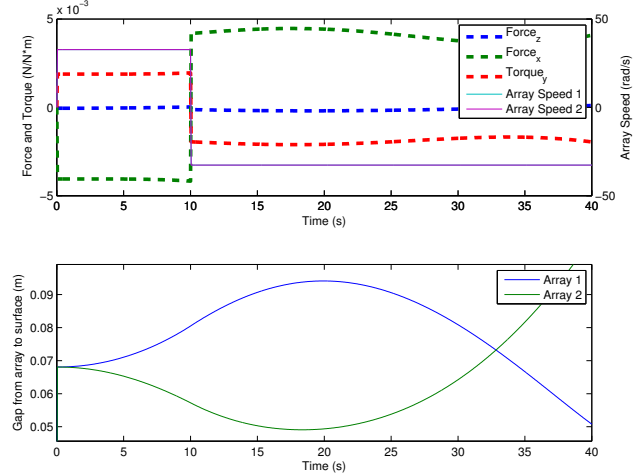


Fig. 8. Simulation of out-of-plane rotation. The top figure shows the input speeds for each coupler and the resultant force and torque on the inspector. The bottom figure shows how the gap between each coupler and the surface change in response to the control forces and torques

V. EXPERIMENTAL DEMONSTRATION

This section presents an experimental demonstration of each motion primitive - planar translation, planar rotation, out-of-plane translation, and out-of-plane rotation in an ideal situation. We constructed two prototype inspection vehicles, each with two spinning magnet arrays - one to demonstrate planar movement shown in figure 9, one to demonstrate out of plane movement shown in figure 1. These inspection vehicles operated on a low-friction air-bearing test bed which allowed them to simulate a space environment with 3 degrees of freedom.

Hardware: The induction couplers were DC hobby gear motors, each with laser-cut cylinder containing a north and south facing 1/2 inch neodymium magnet. A 12V lead-acid battery provided power to the motors, whose power consumption and maximum speed are in table I. An Arduino

microprocessor and Xbee radio enabled remote open-loop commands and handled low-level motor control and a visual tag-based tracking system recorded the vehicle's heading and position with respect to the tags visible in figures 1 and 9.

Considerations: The arrays could not be placed symmetrically about the center of mass due to the constraints of the test platform. Similarly, the tracking points could not be located at the center of mass because the target occulted it from the tracking system, because the target plate was mounted directly above the vehicle out of necessity. These constraints mean that the experiments serve as a demonstration of the motion, rather than a full model validation.

A. Planar Movement

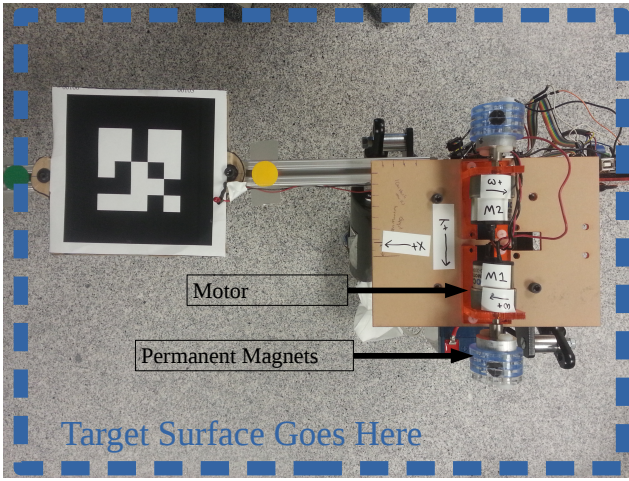


Fig. 9. Overhead view of the platform for demonstrating induction-coupler-generated planar motion

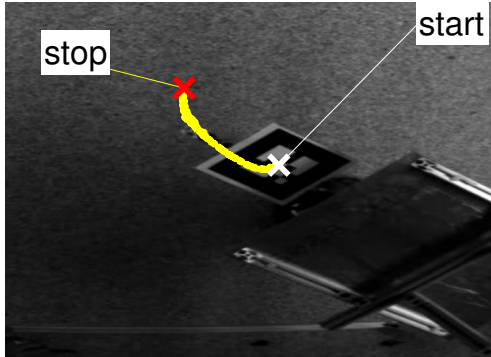


Fig. 10. Trajectory during a planar translation manoeuvre. The body of the inspector is obscured by the target surface in the lower right part of the picture

Figure 10 shows the trajectory of the inspector during planar translation. The inspector spins both arrays forward to translate forward. The majority of the inspector is obscured because the arrays needed to remain directly under the target surface.

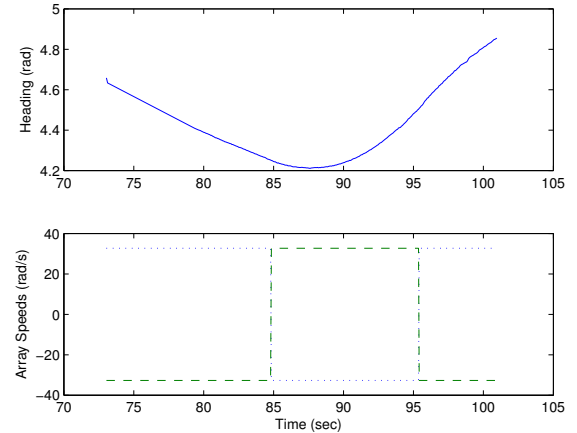


Fig. 11. Inspector heading (top) and induction coupler speed (bottom) during open-loop planar rotation

Figure 11 shows a maneuver in which the inspector used induction couplers to rotate itself around the $-z$ axis and then reversed its motion by generating torque around $+z$. Note that $\dot{\alpha}_1 = \dot{\alpha}_2$, the opposite of the simulations.

B. Out-of-Plane Movement

The plate used to demonstrate out-of-plane movement has a curvature designed to match the harmony module of the ISS. The inspector has two arrays, both with axes pointing in the $-y$ direction, out of the page.

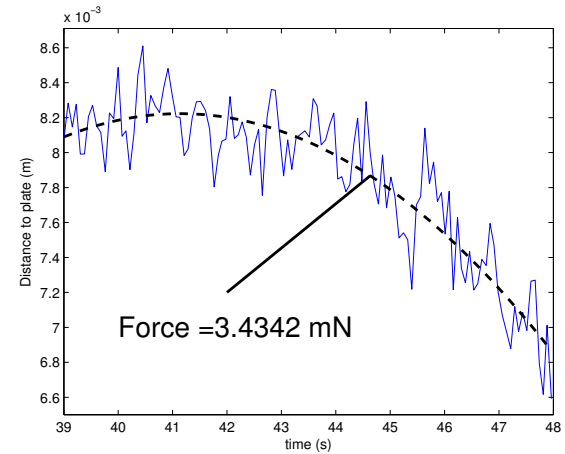


Fig. 12. Distance between plate and center of tag during out-of-plane translation. A quadratic fit finds an estimated force of 3.4 mN

Figure 12 shows the results from the inspector pulling itself towards the surface. The distance it could travel before colliding with the plate was tiny - a clear reason for closed-loop control. The bottom half of the figure shows the inspector accelerating towards the surface - the distance between the CoM and the plate decreases with an increasing rate.

Figure 13 shows the heading of the inspector as it rotates itself out of the plane about the \hat{y} axis.

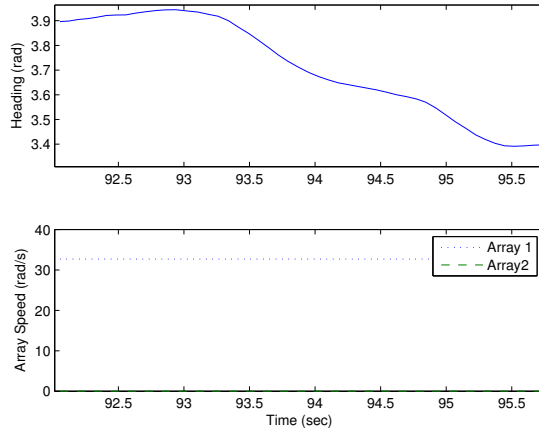


Fig. 13. Inspector heading (top) and coupler speeds (bottom) during out-of-plane rotation

VI. CONCLUSION

This paper focused on modelling and demonstrating the ability of a system of induction couplers to actuate an orbital inspection vehicle in six degrees of freedom near a conductive surface. Contactless, propellantless motion on orbit is unique capability that can form the basis of orbital servicing missions. The construction of a generalized model enables fast dynamic simulations of an inspector using multiple induction couplers to actuate near a target surface. These couplers enable four different open-loop manoeuvres that together span 6-DoF: planar translation, planar rotation, out-of-plane translation and out-of-plane rotation.

Couplers rotating on axes parallel to the plane generate planar motion similarly to a differential drive. Two or more couplers can take advantage of the surface geometry to generate motion out of the plane parallel to the target. This arrangement generates forces in the \hat{z} direction by two or more creating shear forces whose \hat{x} and \hat{y} components cancel but whose \hat{s} components add. Flipping the direction of only one of these couplers produces a torque coupled with a force, enabling rotation out of the plane. Simulations demonstrate each of these four manoeuvres in an ideal scenario and a prototype system on a low-friction air table shows that they work in practice as well as theory.

Future work will focus on two areas - adaptive controllers and movement planning. A robotic inspector will need adaptive controllers to account for induction coupler's strong dependence on poorly known parameters of the environment. The inspector will also need to plan movements carefully because its ability to exert control with an induction coupler is based on both its state and the local geometry.

ACKNOWLEDGMENT

This work was supported by NSTRF Grant #NNX11AN46H.

Thanks to the SPHERES team at NASA Ames for the test-bed and patient support.

REFERENCES

- [1] Rob Ambrose, Brian Wilcox, Ben Reed, Larry Matthies, Dave Lavery, and Dave Korsmeyer. Robotics, Tele-Robotics and Autonomous Systems Roadmap. Technical report, NASA, 2012.
- [2] Jonathan Bird and TA Lipo. Calculating the forces created by an electrodynamic wheel using a 2-D steady-state finite-element method. *Magnetics, IEEE Transactions on*, 44(3):365–372, 2008.
- [3] E Coleshill, L Oshinowo, R Rembala, B Bina, D Rey, and S Sindlar. Dextre: Improving maintenance operations on the International Space Station. *Acta Astronautica*, 64(9-10):869–874, 2009.
- [4] A Ellery. An engineering approach to the dynamic control of space robotic on-orbit servicers. *Proceedings of the Institution of Mechanical Engineers, Part G: Journal of Aerospace Engineering*, 218(2):79–98, 2004.
- [5] A Ellery, J Kreisel, and B Sommer. Ellery, A, J Kreisel, and B Sommer. 2008. The Case for Robotic on-Orbit Servicing of Spacecraft: Spacecraft Reliability Is a Myth. *Acta Astronautica* 63 (5-6): 632648. doi:10.1016/j.actaastro.2008.01.042. ;Go to ISI;://WOS:000258632900010.The case for r. *Acta Astronautica*, 63(5-6):632–648, 2008.
- [6] Gennady Markelov, Rolf Brand, Georg Ibler, and Wolfgang Supper. Numerical assessment of plume heat and mechanical loads and contamination on multi-layer insulation in hard vacuum. *Vacuum*, 86(7):889–894, 2012.
- [7] S. Ali a. Moosavian and Evangelos Papadopoulos. Free-flying robots in space: an overview of dynamics modeling, planning and control. *Robotica*, 25(05):537–547, March 2007.
- [8] Thai-Chau Nguyen-Huynh and Inna Sharf. Adaptive reactionless motion for space manipulator when capturing an unknown tumbling target. *2011 IEEE International Conference on Robotics and Automation*, pages 4202–4207, May 2011.
- [9] Takahisa Ohji, Takashi Shinkai, Kenji Amei, and Masaaki Sakui. Application of Lorentz force to a magnetic levitation system for a non-magnetic thin plate. *Journal of Materials Processing Technology*, 181(1-3):40–43, January 2007.
- [10] Nirmal Paudel and Jonathan Z. Bird. Modeling the Dynamic Electromechanical Suspension Behavior of an Electrodynamic Eddy Current Maglev Device. *Progress In Electromagnetics Research B*, 49(February):1–30, 2013.
- [11] Nirmal Paudel and JZ Bird. General 2-D Steady-State Force and Power Equations for a Traveling Time-Varying Magnetic Source Above a Conductive Plate. *Magnetics, IEEE Transactions on*, 48(1):95–100, 2012.
- [12] P C Rem and P A Leest. A model for eddy current separation. 16(96), 1997.
- [13] J H Saleh, E Lamassoure, and D E Hastings. Space systems flexibility provided by on-orbit servicing: Part 1. *Journal of Spacecraft and Rockets*, 39(4):551–560, 2002.
- [14] W.R Smyth. *Static & Dynamic Electricity*. 5th editio edition, 1989.